# NEARBY MOLECULAR CLOUDS. I. OPHIUCHUS-SAGITTARIUS, $b > 10°$

F. Lebrun[1] and Y.-L. Huang
Goddard Institute for Space Studies
*Received 1982 June 22; accepted 1983 December 9*

## ABSTRACT

Emission from the $1 \rightarrow 0$ transition of carbon monoxide has been mapped over an area of 370 square degrees at $10° < b < 24°$ in the Ophiuchus-Sagittarius region. This survey reveals the existence of an extended complex of molecular clouds, very close to the Sun and probably linked to the Aquila Rift, the $\rho$ Ophiuchi Cloud, and more generally to the Gould Belt. The presence of this complex explains naturally, as a result of $H_2$ formation, the deficiency of atomic hydrogen with regard to both the interstellar absorption and the $\gamma$-ray intensity observed in this region. The correlation between the H I deficiency and the integrated CO line intensity allows one to infer molecular hydrogen column densities.

*Subject headings:* galaxies: Milky Way — galaxies: structure — interstellar: molecules

## I. INTRODUCTION

Heiles (1976) and Burstein and Heiles (1978) studied the relationship between galaxy counts, interstellar reddening, and atomic hydrogen column density [$N$(H I)]. They found that the ratio between $N$(H I) and the interstellar absorption ($A_{pg}$)—as traced by galaxy counts—is nonuniform over the sky. Some regions where this ratio is low correspond to well-known molecular complexes, namely Orion, Taurus, Perseus, and $\rho$ Ophiuchi, where with a constant gas-to-dust ratio, the H I deficiency can be well accounted for by molecular hydrogen formation. The lowest values of $N$(H I)/$A_{pg}$ are located inside the Ophiuchus-Sagittarius region where they cover a large area in the north ($b > 10°$) but are also clearly visible in the south ($b < 10°$) where no molecules are known to exist. Burstein and Heiles (1978) concluded that these low $N$(H I)/$A_{pg}$ values are not only the result of $H_2$ formation but represent real gas-to-dust ratio variations. However, the molecular content of this region is not well known, especially on a large scale.

Strong and Lebrun (1982) proposed to interpret the H I deficiencies in terms of molecular hydrogen so far unobserved. Lebrun and Paul (1983) noted that in the same region, H I is also deficient compared to the $\gamma$-ray intensity observed by *SAS 2* and concluded that there exists $\gamma$-ray–emitting material linked to the dust, this material being most likely molecular hydrogen. This conclusion is also supported by the *COS B* $\gamma$-ray observations (Strong et al. 1982).

At this point, direct observations of molecules seemed necessary (Burstein and Heiles 1982). Because $H_2$ is not directly observable for $A_{pg} > 2$ mag, CO has been used as a tracer of $H_2$. We have undertaken a systematic survey in the CO ($1 \rightarrow 0$) line of the regions showing this H I deficiency and not already known as molecular complexes. This first paper deals with results obtained in the northern part of Ophiuchus and Sagittarius and describes in detail the observational procedure and the data processing. Forthcoming papers will present the results obtained in other regions.

## II. OBSERVATIONS AND DATA PROCESSING

The observations were performed during the winter of 1980–1981 with the 1.2 m millimeter-wave telescope at Columbia University. The telescope has a full beamwidth at half-power of 8' at the frequency of the CO: $1 \rightarrow 0$ transition (115 GHz); however, a faster coverage of the sky can be obtained by degrading the resolution of the experiment. This is achieved by moving the antenna around the observed position during the signal integration (Dame and Thaddeus 1983). A few spectra (10) were recorded at the beginning of the observations with a resolution of 1°. Afterwards a resolution of half a degree was adopted, and all square degrees were covered by four consecutive observations. The spectrometer consists of a 256 channel filterbank, each 250 kHz wide, giving a velocity resolution of 0.65 km s$^{-1}$ at the CO frequency. The frequency switching mode was adopted with a shift of 5 MHz, so that a line and its image are separated by 10 MHz (26 km s$^{-1}$). Although this wide shift produces complicated baseline shapes, it reduces the possibility of blending one line with the image of another. Another problem with the frequency switching mode is the pollution of the spectra by the atmospheric CO emission. However, the velocity of the atmospheric CO line is known *a priori*, and its width and intensity can be found *a posteriori* by analyzing the whole data set (see Appendix A), so that, first of all, each spectrum can be corrected for it.

Since the presence of molecules in this region has been subject to some debate, the data processing procedure was chosen with the intent of making it as objective as possible. In particular the choice of the channels which should be excluded from the baseline fitting of a single spectrum generally relies on a somewhat subjective decision about the existence, position, and width of a line. The aim of the procedure adopted here is to reduce this difficulty by using more information in determining the line parameters.

As a first step, a baseline was fitted to the central part of each spectrum. Only channels at either end of each 256 channel spectrum were excluded from this first baseline fit. To preserve the objectivity of this step, the frequency interval concerned by the baseline fit has to be the same for all spectra, thus rather wide. If we consider that the velocity interval deemed to contain emission is $-20$ to $+20$ km s$^{-1}$ and taking into account the shift in frequency, the baseline fit has to be applied to 100 channels (66 km s$^{-1}$). On such a width, the baseline is adequately described by a fifth order polynomial (see Appendix B). In the second step, $(l,b)$ contour maps of antenna temperature ($T_A^*$) are formed and are used to indicate which
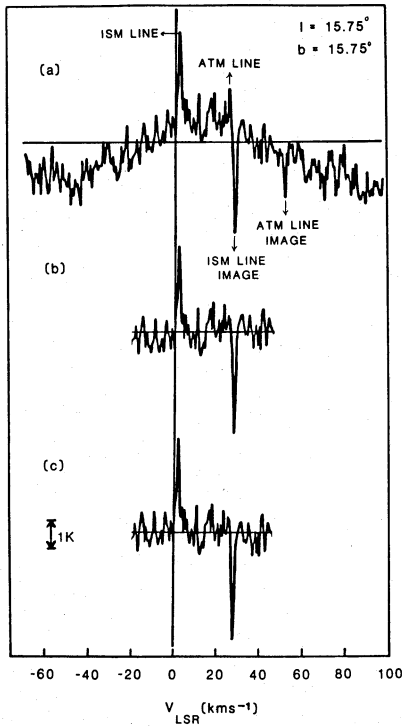
FIG. 1.—Illustration of the data processing: (a) a raw spectrum, (b) the same after the atmospheric line and the first baseline correction, and (c) the same after the second baseline correction.

spectra have to be averaged to optimize the signal-to-noise ratio. During this step, an eye estimate of the noise level is provided by the comparison of the two maps recorded 10 MHz apart. These two maps represent two semi-independent (the atmospheric line could affect both maps) and objective measures of the sky at a given frequency. On this basis the existence of a cloud can be decided with greater confidence than from the examination of each spectrum separately. Finally, for each spectrum, the channels containing the lines accepted from examination of the contour plots were excluded from a new baseline fit, which was then subtracted from the spectrum. The effect of the whole procedure on a sample spectrum is illustrated in Figure 1. Since no emission was found outside the velocity range $-5$ to $+10$ km s$^{-1}$, a folding of the data was applied over that range: $T_A^*(v) = \frac{1}{2}[T_A^*(v) - T_A^*(v + dv)]$, with $dv = 26$ km s$^{-1}$. The resulting

map of the integrated CO line intensity ($W_{CO} = \int T_A^* dv$) is shown in Figure 2.

### III. RESULTS AND DISCUSSION

The molecular clouds found here (see Fig. 2) appear as an extension toward higher latitudes of the very extended CO complex associated with the Aquila Rift (Dame and Thaddeus 1983). The eastern clouds have the same velocity as this complex (6–7 km s$^{-1}$), while the western ones have the same velocity ($\sim 3$ km s$^{-1}$) as the $\rho$ Oph cloud complex which is 15° away. These clouds are located in or near the plane of the Gould Belt, as described by Stothers and Frogel (1974). Moreover, although there is some velocity dispersion, the northern clouds having the lowest velocities ($\sim 0$ km s$^{-1}$), the average velocity of these clouds matches that of the H I feature A of Linblad *et al.* (1973) which is clearly associated with the Gould Belt (see, e.g., Olano 1982 and references therein).

The distance of these clouds can be estimated by the distribution of the interstellar reddening material along the line of sight. In the study of OB stars in the solar neighborhood by Lucke (1978), this region stands out as having the highest reddening per unit distance of the entire sky. The reddening distribution suggests that the complex lies between 50 and 375 pc from the Sun. On the basis of the study by Knude (1978) of the reddening of A and F stars, Arnaud *et al.* (1980) derived a distance consistent with Lucke's estimate. This result is illustrated in Figure 3, where the reddening versus distance relation has been plotted for the 15 stars studied by Knude and located in the region we have observed. It appears that the reddening begins at about 80 pc and extends at least up to 150 pc. Therefore this cloud complex seems to be one of the closest to the Sun. The fact that at these latitudes it is unlikely that a line of sight intercepts any other cloud, makes it a good candidate for detailed study.

Although the presence of a CO complex strongly suggest that H$_2$ formation is responsible for the H I deficiency with regard to both the $\gamma$-ray intensity and the interstellar absorption, a detailed quantitative comparison of the spatial distributions of $N$(H I), $A_{pg}$, and $W_{CO}$ would be appropriate. Unfortunately, because of their poor statistics in this region, galaxy counts are unable to provide an accurate map of the interstellar absorption. On the other hand, the star counts of van Hoof (1969) overlap the present observations by some 126 square degrees. It should be noted that star counts are well adapted to the study of such a closeby complex, the vast majority of the visible stars lying behind it. Using van Rhijn
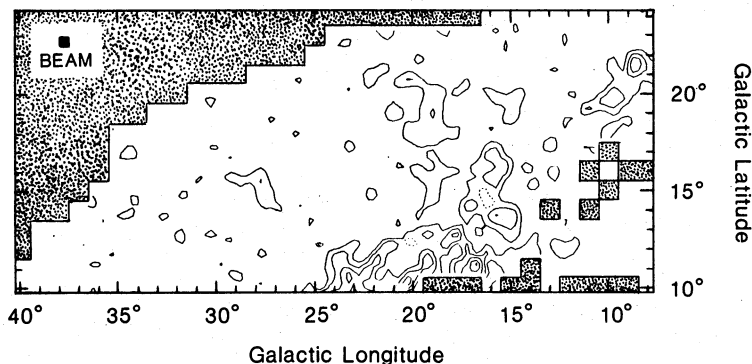


FIG. 2.—Contour map of the integrated CO line intensity, $W_{CO}$. The contour interval is 2.5 K km s$^{-1}$. The shaded areas indicate unobserved regions.
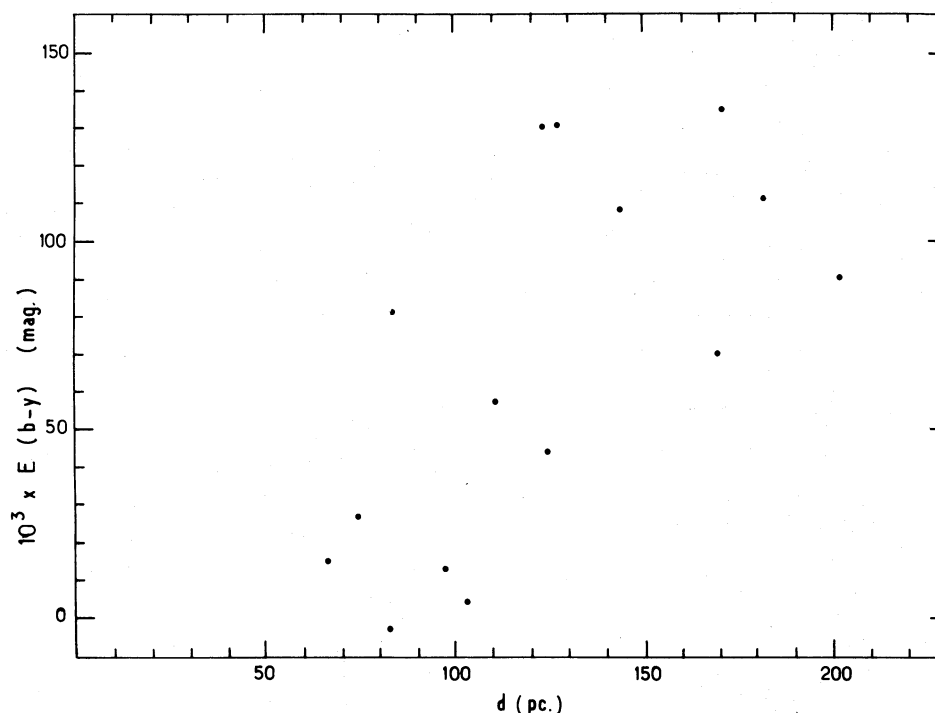
FIG. 3.—The reddening versus distance relation for the 15 stars observed by Knude (1978) lying in the region observed in CO

tables (1935), a 1 square degree resolution map of the inter-stellar absorption has been derived from van Hoof star counts. This is essentially the same as that of Rossano (1978). Assuming H I is optically thin in this region, a comparable map of the H I column density has been derived from the 21 cm survey of Heiles and Habing (1974). The CO data have also been reduced to the same angular resolution (1°). This data base allows one to test the independence of the H I deficiency (defined as: $DN(\text{H I}) = (y/R)A_{pg} - N(\text{H I})$, where $y = [N(\text{H I}) + 2N(\text{H}_2)]/E(B-V) = 5.8 \times 10^{21}$ cm$^{-2}$ mag$^{-1}$ (Bohlin, Savage, and Drake 1978) and $R = A_{pg}/E(B-V) = 4$) and $W_{CO}$. Although both $N(\text{H I})$ and $A_{pg}$ are subject to zero errors (21 cm stray radiation, star number density in the absence of absorption), their scaling, and thus that of $DN(\text{H I})$, is most likely unbiased.

The correlation between $DN(\text{H I})$ and $W_{CO}$ is illustrated in Figure 4. A statistical test of the independence of $W_{CO}$ and $DN(\text{H I})$ can be performed. The coefficient of linear correlation between $W_{CO}$ and $DN(\text{H I})$ is 0.47; with 126 points, the probability of exceeding such a value if $W_{CO}$ and $DN(\text{H I})$ are uncorrelated is $\leq 10^{-7}$. Therefore the H I deficiency is correlated with CO and is likely due to the formation of molecular hydrogen. In order to check if H$_2$—as traced by CO—is chiefly responsible for the apparent variations of the gas-to-dust ratio, we have performed an unweighted multi-linear fit to the data: $A_{pg} = A + B[N(\text{H I}) + CW_{CO}]$. The results are $A = -0.23$ mag, $B = 7.4 \times 10^{-22}$ mag cm$^{-2}$, and $C = 1.3 \times 10^{20}$ cm$^{-2}$ K$^{-1}$ km$^{-1}$ s. The parameter $B$ is a measure of the gas-to-dust ratio: $y = R/B = 5.4 \times 10^{21}$ cm$^{-2}$ mag$^{-1}$, in very good agreement with the standard value. It therefore can be argued that the gas-to-dust ratio in this region is normal, its apparent variations being entirely due to H$_2$ which is well traced by $W_{CO}$. The parameter $C = DN(\text{H I})/W_{CO}$ contains potentially a calibration of $N(\text{H}_2)$ estimates from CO measurements: $X = N(\text{H}_2)/W_{CO} = C/2 = 0.64 \times 10^{20}$ cm$^{-2}$ K$^{-1}$

km$^{-1}$ s. However, this value depends on that assumed for the gas-to-dust ratio. This being the case, it is wise to use the standard value of the gas-to-dust ratio, as was done in deriving the data points of Figure 4, to recalibrate $X$. A more signifi-cant result can be obtained with a fit to these data. The typical error on $W_{CO}$ (averaged over 1 square degree) is about 0.5–0.6 K km s$^{-1}$ ($\sim 10\%$ of the $W_{CO}$ dynamical range), so that even negative values (see Fig. 4) can occur in regions of weak emission. The error on $N(\text{H}_2)$, mainly induced by that on $A_{pg}$, can be estimated to lie in the range $10–15 \times 10^{19}$ cm$^{-2}$ which represents about 15% of the dynamical range of $N(\text{H}_2)$. Therefore the standard least squares fitting procedure, which assumes that all errors can be ascribed to one of the variables, is not applicable here. We have thus adopted the least squares fitting procedure of Worthing and Geffner (1946) which takes into account the relative errors of both variables. This results in $N(\text{H}_2) = (1.1 \pm 0.1)W_{CO}(10^{20}$ cm$^{-2})$. However, because of our poor knowledge of the uncertainties on $N(\text{H}_2)$, both random and systematic (e.g., those on the gas-to-dust ratio), the formal error quoted above is underestimated. A conserva-tive estimate of the $X$ parameter would be: $X = (1.1 \pm 0.5) \times 10^{20}$ cm$^{-2}$ K$^{-1}$ km$^{-1}$ s.

This parameter has been derived recently from a comparison of CO, H I, and $\gamma$-rays from the first galactic quadrant (Lebrun et al. 1983). The derived value, $X = (1–3) \times 10^{20}$ cm$^{-2}$ K$^{-1}$ km$^{-1}$ s, although representing some galactic average between local and remote regions and applying probably to denser media, is not inconsistent with the present estimate. The ratio $\langle N(\text{H}_2)\rangle/\langle W_{CO}\rangle$ for positions with measured extinctions in Dickman's (1978) data is $2 \times 10^{20}$ cm$^{-2}$ K$^{-1}$ km$^{-1}$ s (Liszt 1982). Here again, this value applies to regions denser than those used in the present derivation ($A_{pg} < 2$ mag) and, as noted by Liszt, there is a clear tendency for $X$ to increase with $A_{pg}$. For $A_{pg} < 2$ mag, Dickman's data yields $\langle N(\text{H}_2)\rangle/\langle W_{CO}\rangle = 1.1 \times 10^{20}$ cm$^{-2}$ K$^{-1}$ km$^{-1}$ s,
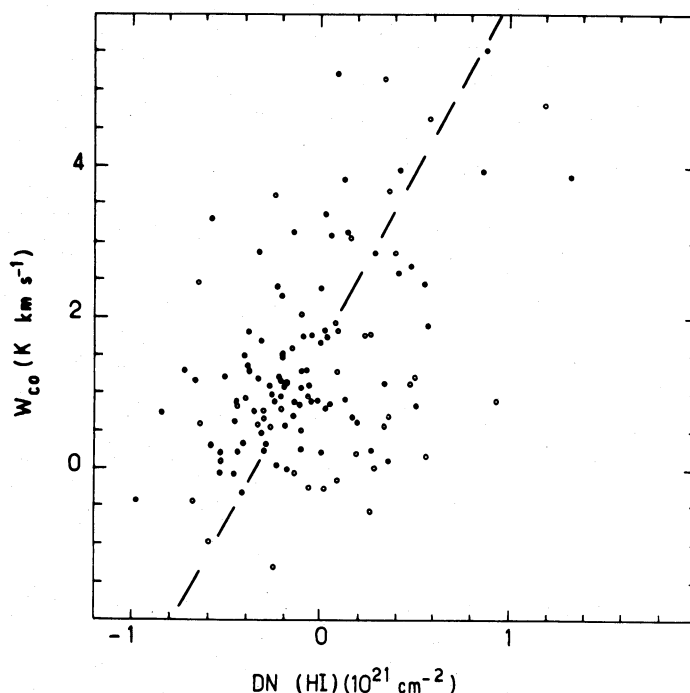
FIG. 4.—The $W_{CO}$ versus $DN(H\,I)$ relation for the 126 points which have been observed in CO and for which star counts are available

in very good agreement with the present determination. In fact the variation of $W_{CO}$ with $N(H_2)$ seems to be primarily governed by CO optical depth effects, $W_{CO}$ not increasing any more for $N(H_2) > (2-3) \times 10^{21}$ cm$^{-2}$. This behavior leads to an increase of $X$ with $N(H_2)$. However, for the densities considered here, the $X$ value should be approximately constant, allowing a determination of molecular hydrogen column densities. With $W_{CO}$ values up to 10 K km s$^{-1}$, in the region observed, we expect $H_2$ column densities up to $1 \times 10^{21}$ cm$^{-2}$, which represents only a fraction of the total gas column density.

Finally, although the whole complex is quite extended, it is probably not very massive. If we adopt $X = 1 \times 10^{20}$ cm$^{-2}$ K$^{-1}$ km$^{-1}$ s and a distance of 100 pc, its $H_2$ mass is a few $10^3 M_\odot$. Such a complex would probably better be designated as a complex of diffuse clouds. In this regard, the lack of young objects (OB stars, T Tauri stars, H II regions) commonly associated with dense molecular clouds is not so surprising.

## APPENDIX A

At the end of this survey of about 3300 spectra, the atmospheric CO line was analyzed. Its shape was found to be close to a Lorentzian profile whose width (0.3 MHz) indicates a pressure reached at about 65 km height (Waters, Wilson, and Shimabukuro 1975). Its average intensity appears to vary linearly with the cosecant of the elevation. The intensity of the line normalized to the zenith also varies from day to day. With a good accuracy compared to the noise level, the intensity of the line in a given spectrum can be predicted:

$$I_j = \mathrm{cosec}\,(\alpha_j)(\textstyle\sum I_i)/\sum \mathrm{cosec}\,(\alpha_i) \,,$$

where $N$ is the number of spectra taken on the same day and $\alpha$ is the elevation at which the spectrum was recorded. The first step of the data processing was then the subtraction of the predicted atmospheric line from each spectrum.

## APPENDIX B

The use of a fifth-order polynomial for the baseline fit requires some justification. It should be noted that such a fit applied to 100 channels (94 degrees of freedom) is equivalent to fit separately the line and image baselines over 50 channels with a parabola. As mentioned in the text, the comparison of a line and its image gives an estimate of the rms noise in the data:

$$S = \left\{ \left[ \sum_{i=1}^{N} \sum_{j=1}^{M} (T_{i,j} + T_{i,j+k})^2 \right] \Big/ 2NM \right\}^{1/2} ,$$

where $N$ is the number of spectra, $M$ is the number of channels used in each spectrum, and $k$ is the number of channels of the frequency shift (40). It turns out that after the atmospheric line correction, the first baseline correction and before folding, $S$, computed for the 330 spectra for $-5 < v < 10$ km s$^{-1}$ (23 channels) is about 0.43 K. For comparison, the use of linear baseline corrections for the line $(-5 < V < 10$ km s$^{-1})$ and the image $(21 < V < 36$ km s$^{-1})$ for 10 spectra showing emission leads to $S = 0.53$ K. Bearing in mind that this last baseline fit has only 42 degrees of freedom (46 data points, 4 parameters), such a difference justifies the use of a higher order polynomial for the baseline fit.

REFERENCES

Arnaud, M., Rocchia, R., Rothenflug, R., and Soutoul, A. 1980, *Proc. 17th Int. Cosmic Ray Conf.* (Paris), **1**, 131.
Bohlin, R. C., Savage, B. D., and Drake, J. F. 1978, *Ap. J.*, **224**, 132.
Burstein, D., and Heiles, C. 1978, *Ap. J.*, **225**, 40.
———. 1982, *A.J.*, **87**, 1165.
Dame, T. M., and Thaddeus, P. 1983, in preparation.
Dickman, R. L. 1978, *Ap. J. Suppl.*, **37**, 407.
Heiles, C. 1976, *Ap. J.*, **204**, 379.
Heiles, C., and Habing, H. J. 1974, *Astr. Ap. Suppl.*, **14**, 1.
Knude, J. 1978, *Astr. Ap. Suppl.*, **33**, 347.
Lebrun, F., and Paul, J. A. 1983, *Ap. J.*, **266**, 276.
Lebrun, F., *et al.* 1983, *Ap. J.*, **274**, 236.
Linblad, P. O., Grape, K., Sandquist, Aa., and Schober, J. 1973, *Astr. Ap.*, **24**, 309.

Liszt, H. S. 1982, *Ap. J.*, **262**, 198.
Lucke, P. B. 1978, *Astr. Ap.*, **64**, 367.
Olano, C. A. 1982, *Astr. Ap.*, **112**, 195.
Rossano, G. S. 1978, *A.J.*, **83**, 241.
Stothers, R., and Frogel, J. A. 1974, *A.J.*, **79**, 456.
Strong, A. W., and Lebrun, F. 1982, *Astr. Ap.*, **105**, 159.
Strong, A. W., *et al.* 1982, *Astr. Ap.*, **115**, 404.
van Hoof, A. 1969, *Bull. Astr. Inst. Netherlands Suppl.*, **3**, 137.
van Rhijn, P. J. 1929, *Pub. Kapteyn Astr. Lab.*, **43**.
Waters, J. W., Wilson, W. J., and Shimabukuro, F. I. 1975, *Science*, **191**, 1174.
Worthing, A. G., and Geffner, J. 1946, *Treatment of Experimental Data* (New York: John Wiley and Sons).

Y.-L. Huang: Goddard Institute for Space Studies, 2880 Broadway, New York, NY    10025

F. Lebrun: CEN-Saclay DphG/SAP 91191, Gif-sur-Yvette, CEDEX, France